# SEGREGATION ARISING FROM NATURAL CONVECTION DURING SOLIDIFICATION

Joseph R. Sarazin and Angus Hellawell

Department of Metallurgical and Materials Engineering
Michigan Technological University
Houghton, MI 49931

## Abstract

Density driven convection during solidification has been recognized for some time to result in macrosegregation particularly when lower density alloying elements are rejected into the interdendritic liquid. The resulting segregates are commonly referred to as channels, freckles or A-segregates. Buoyancy driven convection leading to channel formation has been examined in three model systems possessing somewhat different materials parameters. They are the Pb-Sn eutectic system, the transparent aqueous-salt $NH_4Cl$-$H_2O$ eutectic system and the transparent organic succinonitrile-ethanol monotectic system. Convection in these systems is controlled by a balance of buoyant and viscous forces, which are strong functions of composition and temperature. Composition, temperature and flow velocity were measured and elimination of channels through heavier ternary additions is discussed.

EPD Congress '91
Edited by D. R. Gaskell
The Minerals, Metals & Materials Society, 1991

## Introduction

Natural convection in the liquid during alloy solidification may interact with the growth of a solid phase or phases and lead to morphological changes [1-3] or inhomogeneities in the form of segregation defects [4] in a cast product. Convection in the liquid results from differences in liquid density arising from thermal and/or compositional gradients within the melt with the resulting flow patterns dependent upon the geometry and the sign of the density gradient relative to the direction of the gravitational vector. Even in the absence of gravity, convection may still be present, driven by volume changes on freezing [5-8] or surface tension gradients again due to thermal and/or compositional differences, so-called Marongoni convection [9-10].

Under terrestrial conditions, density driven convection in the liquid generally dominates. In a casting of any appreciable size, temperature gradients (dT/dz) are inevitable (with respect to some arbitrary reference axis) and if an alloy freezes over a significant temperature range, rejection of one or more components from the solid may result in solute gradients (dc/dz) as well. The magnitude and sign of the resulting density gradient ($d\rho/dz$) is dependant upon the respective expansion coefficients $\alpha = d\rho/dT$ and $\beta = d\rho/dc$. $\alpha$ is always positive while $\beta$ may be either positive or negative. Density is, in general a more sensitive function of composition, thus $\beta$ often exceeds $\alpha$ by nearly an order of magnitude. Since $\beta$ can be of either sign, the resulting density driven convective flow patterns can vary from system to system and within a given system, will depend upon the orientation of the growth direction with reference to the gravitational vector.

Figure 1a & b show schematically the flow patterns observed with horizontal growth (perpendicular to the gravitational vector) as in conventional billet or ingot castings while c & d and e & f represent growth antiparallel, (dT/dz positive) and parallel (dT/dz negative) to the gravitational vector respectively, such as in directionally solidified castings or contrived crystal growth situations. Figures on the left a, c, and e have $\beta$ negative i.e. solute additions decrease density while those on the right represent a solute density greater than the solvent ($\beta$ positive). Some form of convection will result in all but 1d where the higher density, solute rich liquid stabilizes the system against convection.

Of particular interest is the configuration in 1c where the temperature and compositional density gradients are opposing with a lower density solute rejected interdendritically. In this case a density inversion in the liquid will result with the lighter, solute rich interdendritic liquid within the mushy zone surmounted by a higher density bulk liquid which is thermally stabilized against convection. The density inversion in this case is accommodated by very localized flow upward in the form of circular plumes or jets emanating from holes or channels within the mushy zone with corresponding re-entrainment of bulk liquid in regions adjacent to the channels. It is these holes or channels which are the last to freeze and are left as defects in the solidified casting.

Figure 2 is a shadowgraph showing those convective plumes in a transparent analogue 30% $NH_4Cl$-$H_2O$ casting while Figure 3 reveals the resulting defects (sectioned perpendicular to the growth direction) in a Pb 10% Sn alloy. These macroscopic defects (on the order of 1 mm wide and up to $10^2$ mm long) are commonly known as channels or freckels when present in directionally solidified ESR ingots [11] or turbine blades [12].

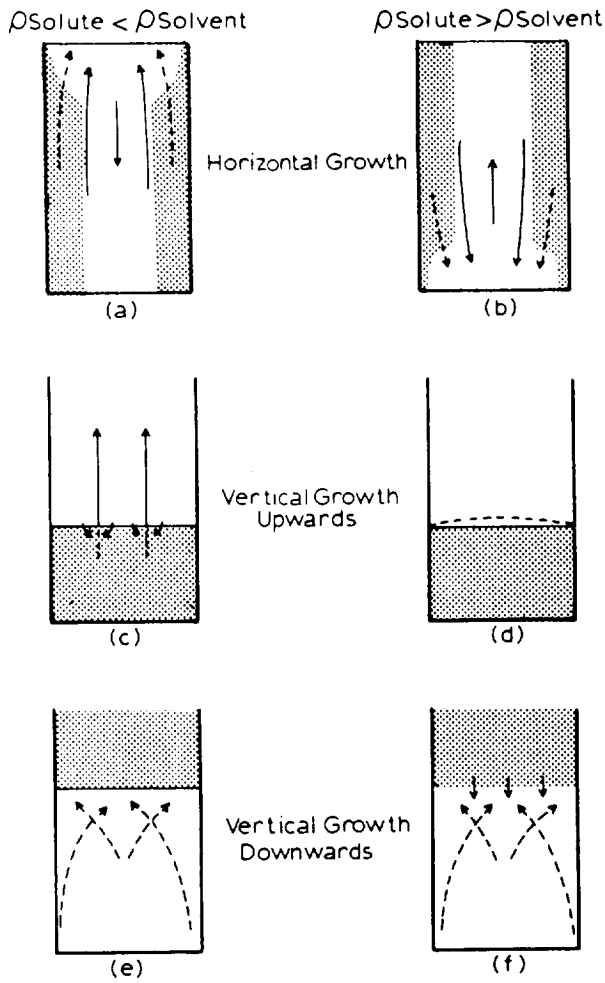


Figure 1 - Buoyancy driven convective flow patterns for alternative heat flow (a & b horizontal, c & d vertical down, and e & f vertical up) and solutal density gradient combinations. (a, c, & e, $d\rho/dc$ (-) and b, d, & f, $d\rho/dc$ (+)).


Figure 2 - Shadowgraph of water rich interdendritic liquid plumes exiting the mushy zone in a 30% $NH_4Cl$-$H_2O$ casting during solidification.

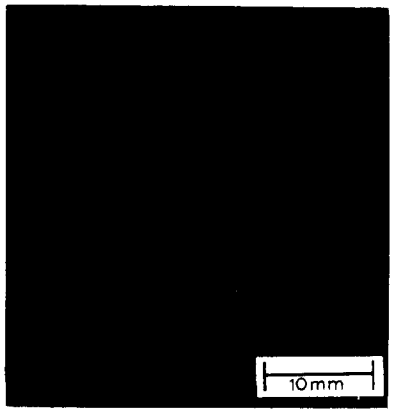


Figure 3 - Sn rich channels or freckels present in a transverse section of a Pb-10 wt.% Sn ingot.

Similar defects arise in the configuration in Figure 1a particularly in steel billet castings [4,13-15] where they are commonly known as "A" segregates, as well as in 1b and f. These configurations, however, are more difficult to study experimentally due to the complications of generalized convective flow in the bulk liquid.

From this point discussion will be confined to the configuration in Figure 1c, i.e. directional growth vertically upward with rejection of a less dense solute.

Its been known for some time that channel or freckels arise from buoyant convection during solidification [11,13,16] what is not so clear is the mechanism by which channel flow originates and the parameters which control the number, size, spatial distribution and flow rate of the resulting channel plumes.

## Flow Initiation

Since channel flow involves both the interdendritic liquid within the semi-permeable mushy zone as well as the bulk liquid ahead of the growth front, the choice of origin is at some depth within the mushy zone or at a position at or ahead of the dendritic front. Although analysis have been formulated for the former [17-19] experimental evidence obtained using transparent metal analogues suggests that flow originates from a liquid disturbance at or just ahead of the growth front [20-21] with subsequent formation of channels backwards into the mushy zone.

Considering solidification vertically upwards of an alloy of composition $C_o$ into a positive gradient as shown schematically in Figure 4, one finds at

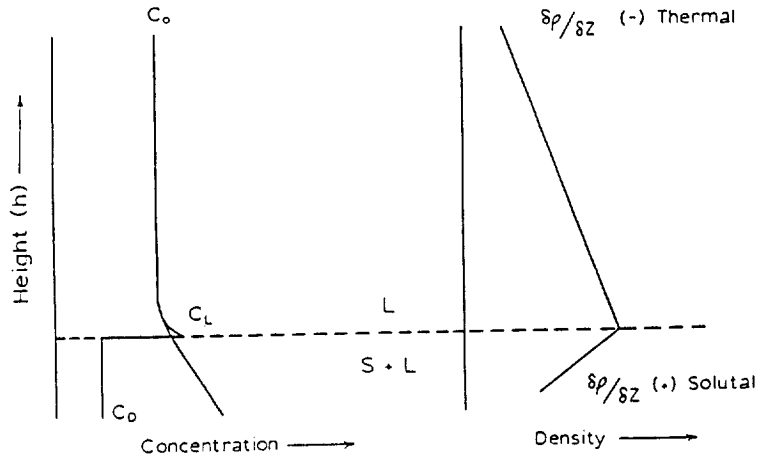


Figure 4 - Schematic concentration and density profiles above and below the dendritic front ($d\rho/dc$ (-), $d/T/dz$ (+)).

the growth front, a slightly enriched boundary layer of composition $C_L$, depositing solid of composition $C_D$, while between the dendrites within the mushy zone the liquid is in local equilibrium with the solid according to temperature and composition along the liquidus line of the phase diagram. If $\beta \times dc/dz$ exceeds $\alpha \times dT/dz$ along the liquidus line, the net density gradient within the mushy zone is positive i.e. inherently unstable while that within the bulk liquid, presumed to be of uniform composition, is negative or stable. Despite the fact that the positive solutal density gradient often exceeds the negative thermal density gradient, convection is not spontaneous since the less dense liquid below must break through the quiescent, supernatent bulk liquid. It is thus evident that liquid perturbations leading to flow must originate at or near the dendritic interface at the level where the density gradient changes sign. Without a perturbation at this level, fluid originating from greater depths cannot be released. Although no formal analysis for breakaway of this boundary layer fluid has been developed, conditions are such that flow will result by thermosolutal convection.

Thermosolutal convection, recognized for some time in oceanographic contexts [22-24] as thermohaline convection is a generic phenomena responsible for convective flow in a wide range of natural systems [23]. Simply stated it is mass transport arising due to a diffusivity difference between heat and solute. In general $D_{thermal} >> D_{solute}$ so that fluid displaced upwards will come to rapid thermal equilibrium but remain solute rich and thereby less dense than its surroundings.

Thermosolutal convection originates when a critical value of a thermosolutal Rayleigh number is exceeded [2,24-26] resulting in a flow pattern with a width scale on the order of the primary dendrite spacing (~ .5 mm) and extending some 2-3 cm ahead of the dendrite interface. The convective cells established have come to be known as "salt fingers". A simple minded analysis of the quantities in a critical thermosolutal Rayleigh number [27-30] shows that if the number were unity, the relevant dimension in the equation, for both metallic and aqueous analogue systems, would be similar to the primary dendrite spacing. Since the liquid perturbations are occurring at the dendritic front with its periodic nature, such a coincidence might well be expected.

For a given alloy system, the primary dendrite spacing is dependant on the temperature gradient (G) and growth velocity (V) (approximating proportional to $G^{-1/2}\ V^{-1/4}$ [31]). It is interesting to note that increases in either G or V both refine dendrite spacing and have been qualitatively observed to decrease the incidence of channel formation, i.e. increases in G and/or V result in a subcritical Rayleigh number, predicting no thermosolutal convection and therefore no mechanism for initiation of channel flow.

In both the $NH_4Cl$-$H_2O$ and succinonitrile-ethanol systems "salt finger" convection has been observed to precede channel formation. By some, as of yet unexplained criteria, certain salt fingers are coupled with flow in the mushy zone to result in channel flow with dimensions on the order of 3-5 times the primary dendritic spacing.

The incidence of channels within a given system also appears to be compositionally dependant. At high solute contents (with a correspondingly open and permeable mushy zone) coupling to form discrete channels does not

occur and convective flow does not progress beyond the salt finger regime. With decreasing solute content under given growth conditions, the onset of channels is initially delayed to longer and longer times eventually reaching a point where the fraction solid within the mushy zone is so high as to make it essentially impermeable. Since re-entrainment of liquid into the mushy zone is necessary for continued flow, there is a lower limit to channel formation within a given system.

## Channel Dimensions and Flow Rates

As was alluded earlier, the quasi-steady state propagation of established channels is separate and subsequent to the initial breakdown and formation of salt fingers. It is interesting that for the three model systems examined (metallic Pb-Sn, aqueous $NH_4Cl$-$H_2O$ and organic succinonitrile-ethanol) that the formation of channels and their dimensions are, to a first approximation, identical despite a rather wide range of physical properties. The relevant physical properties can be conveniently expressed in terms of the dimensionless Prandtl and Lewis numbers ($\sigma$ and $\tau$).

Important quantities for consideration in comparison of channel flow in the three systems are summarized in Table I. Some of the quantities cannot be readily measured, i.e. flow velocities and temperature difference between plumes and bulk in the opaque metallic system. Channel/plume composition differences are averages based on EMPA in Pb-Sn and refractive index measurements of liquid samples in the transparent analogues. Composition and temperature difference data for the organics have yet to be measured.

Since the channel radius and spacing are essentially unchanged from one system to another one might ask what factors determine the relationship between the composition difference ($\Delta C$) driving flow and the resulting plume flow rates? In order to do this we must examine plume flow more closely to determine how the plume flow rate, channel radius and buoyancy forces are tied together. As a first approach, one might consider plume flow to be analogous to flow along a tube. Neglecting end effects, this gives a parabolic velocity distribution in the plume described by the well known Poiseuille equation. This equation however is not strictly applicable due to the imposition of a no slip boundary condition at the walls of the plume. In actuality the moving plume drags along some of the quiescent bulk liquid causing the radial velocity to decay exponentially around the plume, resulting in a velocity distribution shown schematically in Figure 5.

Table I. Relevant Plume Flow Data

| | Metallic | Aqueous | Organic |
|---|---|---|---|
| $\sigma$ | $\sim 2 \times 10^{-2}$ | ~7 | ~21 |
| $\tau$ | $4 \times 10^{3}$ | $10^{2}$ | $10^{2}$ |
| channel radius, r (m) | $6 \times 10^{-4}$ | $6 \times 10^{-4}$ | $6 \times 10^{-4}$ |
| average flow velocity, V (m/sec) | * | $10^{-2}$ | $10^{-3}$ |
| composition difference, $\Delta C$ (wt.%) | 3.5 | .65 | * |
| temperature difference, $\Delta T$(K) | * | 3 | * |
| channel spacing, L(m) | $10^{-1}$ | $10^{-1}$ | $10^{-1}$ |
| fraction liquid in mushy zone, $f_L$ | .08 | .86 | .74 |
| primary spacing, $\lambda$ (mm) | $3 \times 10^{-4}$ | $4 \times 10^{-4}$ | $6 \times 10^{-4}$ |

*no measurements

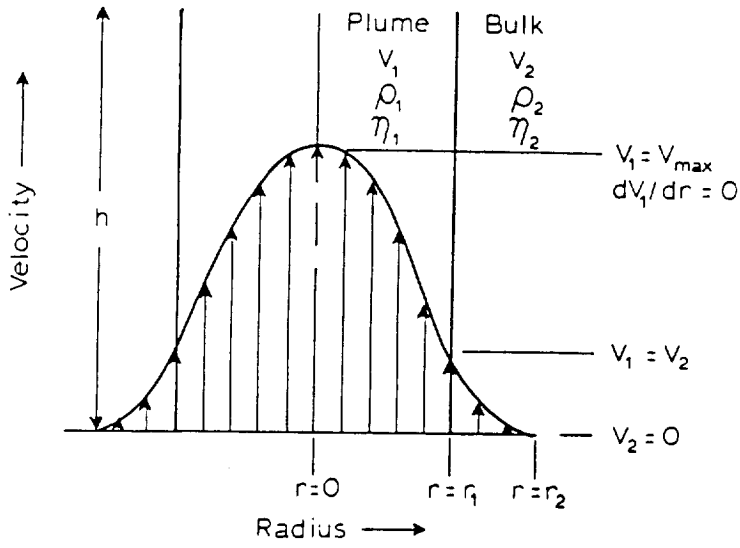


Figure 5 - Schematic of the velocity profile and boundary conditions for flow of a cylindrical plume of liquid through a quiescent liquid of higher viscosity.

The plume "wall" actually represents a region of maximum shear which corresponds to the point at which the refractive index changes most rapidly in a transparent material. The radial velocity distribution in the plume then fits a modified parabolic equation of the basic form:

$$V = \frac{Pr_o^2}{2h\eta}$$

where $r_o$ is the plume radius as defined above, P is the buoyant pressure of the form $\Delta\rho gh$, $\eta$ is the dynamic viscosity and h is the plume height. g is the gravitational constant and $\Delta\rho$ can be given by $\rho\beta\Delta C$ involving the bulk density $\rho$, the solutal expansion coefficient $\beta$ and the mean compositional difference between the plume and surrounding liquid.

If the plume temperature is below that of the bulk (which it is by ~ 1-3 K in the aqueous system) then the buoyant pressure may be reduced by $\alpha\rho\Delta T$ where $\Delta T$ is the temperature difference and $\alpha$ is the thermal expansion coefficient. The basic form of the velocity profile has been described but the criterion is still lacking for the selection process between $r_o$, V or $\Delta C$.

Two possibilities can be considered, first that plume flow is as rapid as is consistent with the observed laminar flow i.e. less than the onset of turbulence as determined by critical Reynolds number $Re = \frac{Vr}{\nu}$ ($\geq 10^3$) where $\nu$ is the kinematic viscosity, or, secondly, that the system comes to thermal equilibrium which would limit flow rates to $V = K/r$ where K is the thermal conductivity, a condition necessary for the formation of steady state "salt

finger" convection which precedes channel flow. Plotting these possible limiting criteria in Figure 6 on a log scale we find the observed rates for the aqueous system to lie well below the laminar to turbulent transition given by Reynolds yet significantly above the rates necessary for complete thermal equilibration, as might be expected since temperature measurements made by passing a fine wire thermocouple through the plumes reveal a net $\Delta T$ between the plume and bulk liquids. The line denoted "Poiseuille" considers the no slip condition at the wall and incorporating slip as in the real case would result in a higher velocity for a given radius, more closely approaching the observed value for the aqueous system. Similar results can be obtained for the organic system but confirmatory observed data for the metallic system is lacking due to the difficulties in measuring flow velocity in the opaque liquid. Extrapolating velocities from the analogue systems using measured $\Delta C$ and r values for the metal system indicate flow velocities in the metal system in excess of 100 mm/sec!

Since neither criteria adequately predicts the observed case it is necessary to go back and re-evaluate the assumption of no end effects, particularly since the bottom end of the plume is embedded in the semi-permeable mushy zone which might be expected to limit the volume of liquid which can be drawn into the channel. Clearly there would be a lower limit to permeability below which a sufficient volume of liquid simply could not be re-entrained to maintain flow for a given buoyancy pressure. In order to quantify this restriction on reentrainment, it is necessary to consider the flow rate and viscosity of the interdendritic liquid as well as the geometry of the dendritic grid within the mushy zone, particularly the number, size and tortuousity of interdendritic liquid "pipes" which feed the channel, as well as to what depth below the front the flow is significant. The fraction of solid within the mushy zone increases with depth, decreasing the

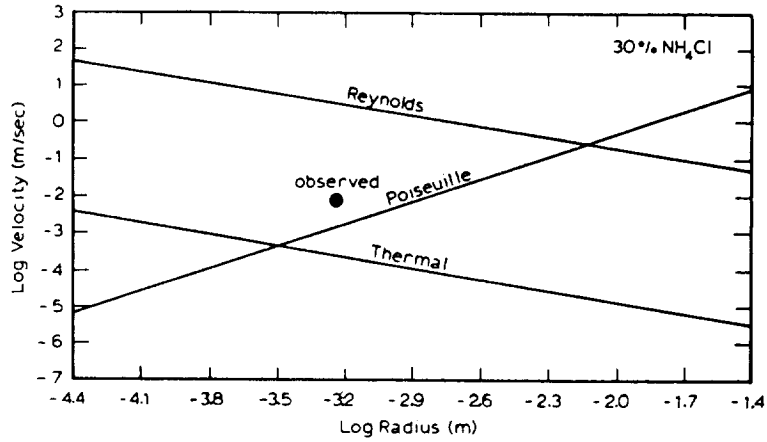


Figure 6 - The flow rate/radius relationships (log $V(m \cdot sec^{-1})$ vs. log r(m)) for a 30% $NH_4Cl$ analogue alloy indicating limiting values for turbulence, [4]pipe flow and thermal equilibrium.

permeability of the mushy zone and limiting the flow contributions at greater depths. Experiments using dye to trace re-entrainment patterns in analogue castings have confirmed significant flow to be limited to a hemispherical volume with a radius of approximately 1/2 the spacing between channels. Measured concentration and temperature differences ($\Delta C$ & $\Delta T$) between the plume and bulk liquids are consistant and when compared with the axial composition and temperature gradients within the mushy zone, verify that plume flow originates close to the dendritic front.

## Channel Elimination

In alloys prone to the formation of these defects, alteration of composition and/or processing technique can eliminate channel formation. As was mentioned earlier, it has been known for some time that increases in temperature gradient and growth velocity [11,16,32] qualitatively decrease the incidence of channel formation. Increasing either parameter decreases the scale and permeability of the mushy zone making channel formation more difficult.

By additions of heavier alloying elements, which also segregate to the interdendritic liquid, it is possible to negate the density difference driving buoyant flow. Ternary additions of $ZnCl_2$ to $NH_4Cl$-$H_2O$ have been shown to reduce the incidence of channel formation [21,33] and efforts are currently underway to systematically eliminate the buoyancy force through ternary additions to aqueous and organic analogue castings.

When little or no flexibility in composition or processing conditions are possible, simple mold movements (i.e. slow rotation about an axis inclined to the vertical) have been shown to eliminate channels [20,21,34]. The effect of such a movement is to cause the bulk liquid to shear continuously past the advancing interface, shearing off any plumes present before they can develop.

## Conclusions

1. Channel segregation results from buoyancy driven convection in the liquid during alloy solidification.

2. Thermosolutal convection leading to channel formation occurs ahead of the dendritic front when a critical value of the thermosolutal Rayleigh number is exceeded.

3. Channels are established by coupling of the thermosolutal convection in the bulk liquid with flow in the mushy zone and subsequent formation of channels backwards from the interface. The criteria for coupling are as yet unknown.

4. The factors which control the composition difference ($\Delta C$), channels radius (r) and flow rate (v) relationships for channel formation are complicated functions involving the interaction of buoyancy, viscosity and approach to thermal equilibrium and the geometrical constraints of the permeability of the mushy zone.

5. Channels can be eliminated by increases in temperature gradient and/or growth velocity, by heavier alloying additions to negate buoyancy or by slow rotation of the casting about an axis inclined to the vertical during solidification.

## Acknowledgments

The authors would like to acknowledge the financial support of the National Aeronautics and Space Administration - Lewis Research Center, Contract #NAG-3-560 and the National Science Foundation, Contract # DMR8815049.

## References

1. M. E. Glicksman, S. R. Coriell, and G. B. McFadden, Ann. Rev. Fluid Mech., 18, 307-335 (1986).

2. D.T.J. Hurle, E. Jakeman, and A. A. Wheeler, J. Crystal Growth, 58, 163-179 (1982).

3. J. D. Verhoeven, J. T. Mason and R. Trivedi, Metall. Trans. A, 17A, 991-1000 (1986).

4. M. C. Flemings, Solidification Processing, McGraw Hill (1974).

5. M. C. Flemings and G. E. Nero, Trans. Met. Soc. AIME, 239, 1449-1460 (1967).

6. M. C. Flemings, R. Mehrabian, G. E. Nero, Trans. Met. Soc. AIME, 242, 41-49 (1968).

7. M. C. Flemings and G. E. Nero, Trans. Met. Soc. AIME, 242, 50-55 (1968).

8. A. L. Maples and D. R. Poirier, Metall. Trans. B, 15B, 163-172 (1984).

9. A. V. Hershey, Physical Review, 56, 204 (1939).

10. L. E. Scriven and C. V. Sternling, Nature, 187, 186-188 (1960).

11. A. F. Giamei and B. H. Kear, Metall. Trans., 1, 2185-2192 (1970).

12. R. L. Dreshfield, Journal of Metals, 39 (7), 16-21 (1987).

13. R. J. McDonald and J. D. Hunt, Metall. Trans., 1, pp. 1787-1788 (1970).

14. F. W. Wienberg, J. Laif, and R. Pugh, Solidification and Casting of Metals, The Metals Society, London Book 192, pp. 334-339 (1979).

15. G. W. Davies, Solidification and Casting, Applied Sciences, London (1973).

16. S. M. Copley, A. F. Giamei, S. M. Johnson, and M. F. Hornbecker, Metall. Trans., 1, 2193-2204 (1970).

17. M. R. Bridge, M. P. Stephenson, and J. Beech, Metals Technology, 9, 429-433 (1982).

18. V. R. Voller, J. J. Moore, and N. A. Shah, Metals Technology, 10, 81-84 (1983).

19. M. Simpson, M. Yerebakan, and M. C. Flemings, Metall. Trans., 16A, 1687-1689 (1985).

20. A. K. Sample and A. Hellawell, Metall. Trans., 13B, 495-561 (1982).

21. A. K. Sample and A. Hellawell, Metall. Trans., 15A, 2163-2173 (1984).

22. M. E. Stern, Tellus, 12, 172-175 (1960).

23. R. W. Schmidt, Phys. Fluids, 26 (9), 2373-2377 (1983).

24. J. S. Turner, Ann. Rev. Fluid Mechanics, 17, 11-44 (1985).

25. S. R. Coriell, M. R. Cordes, W. J. Boettinger, and R. F. Sekerka, J. Crystal Growth, 49 (198), 13-28 (1980).

26. G. R. McFadden, R. G. Rehm, S. R. Coriell, W. Chuck, and K. A. Morrish, Metall. Trans., 15A, 2121-2137 (1984).

27. J. R. Sarazin and A. Hellawell, Advances in Phase Transitions, Pergamon Press, 101-115 (1988).

28. J. R. Sarazin, M. S. Thesis, Michigan Technological University (1986).

29. J. R. Sarazin and A. Hellawell, Metall. Trans., 19A, 1861-1871 (1988).

30. J. R. Sarazin and A. Hellawell, Solidification Processing 87, Institute of Metals, London, 94-97 (1988).

31. W. Kurtz and D. J. Fisher, Fundamentals of Solidification Trans. Tech. Publications, Switzerland (1984).

32. J. R. Sarazin, Ph.D. Thesis, Michigan Technological University (1990).

33. A. K. Sample, M.S. Thesis, Michigan Technological University (1984).

34. A. Hellawell, U. S. Patent #4 462 354, July 1984.